

This is a copy of the published version, or version of record, available on the publisher's website. This version does not track changes, errata, or withdrawals on the publisher's site.

# One-dimensional electronic states in a natural misfit structure

Alla Chikina, Gargee Bhattacharyya, Davide Curcio, Charlotte E. Sanders et.al.

## Published version information

**Citation:** A Chikina et al. One-dimensional electronic states in a natural misfit structure. Phys Rev Materials 6, no. 9 (2022): L092001

**DOI:** [10.1103/PhysRevMaterials.6.L092001](https://doi.org/10.1103/PhysRevMaterials.6.L092001)

This version is made available in accordance with publisher policies. Please cite only the published version using the reference above. This is the citation assigned by the publisher at the time of issuing the APV. Please check the publisher's website for any updates.

This item was retrieved from **ePubs**, the Open Access archive of the Science and Technology Facilities Council, UK. Please contact [epublications@stfc.ac.uk](mailto:epublications@stfc.ac.uk) or go to <http://epubs.stfc.ac.uk/> for further information and policies.

## One-dimensional electronic states in a natural misfit structure

Alla Chikina,<sup>1</sup> Gargee Bhattacharyya<sup>2</sup>,<sup>3</sup> Davide Curcio<sup>4</sup>,<sup>1</sup> Charlotte E. Sanders,<sup>3</sup> Marco Bianchi,<sup>1</sup> Nicola Lanatà<sup>4</sup>,  
Matthew Watson,<sup>5</sup> Cephise Cacho,<sup>5</sup> Martin Bremholm,<sup>6</sup> and Philip Hofmann<sup>1,\*</sup>

<sup>1</sup>*Department of Physics and Astronomy, Interdisciplinary Nanoscience Center (iNANO), Aarhus University, 8000 Aarhus C, Denmark*

<sup>2</sup>*Department of Physics and Astronomy, Aarhus University, 8000 Aarhus C, Denmark*

<sup>3</sup>*Central Laser Facility, STFC Rutherford Appleton Laboratory, Harwell OX11 0QX, United Kingdom*

<sup>4</sup>*School of Physics and Astronomy, Rochester Institute of Technology, Rochester, New York 14623, USA*

<sup>5</sup>*Diamond Light Source, Division of Science, Didcot OX11 0QX, United Kingdom*

<sup>6</sup>*Department of Chemistry, Interdisciplinary Nanoscience Center (iNANO), Aarhus University, 8000 Aarhus C, Denmark*



(Received 29 April 2022; revised 14 July 2022; accepted 12 September 2022; published 28 September 2022)

Misfit compounds are thermodynamically stable stacks of two-dimensional materials, forming a three-dimensional structure that remains incommensurate in one direction parallel to the layers. As a consequence, no true bonding is expected between the layers, with their interaction being dominated by charge transfer. In contrast to this well-established picture, we show that interlayer coupling can strongly influence the electronic properties of one type of layer in a misfit structure, in a similar way to the creation of modified band structures in an artificial moiré structure between two-dimensional materials. Using angle-resolved photoemission spectroscopy with a micron-scale light focus, we selectively probe the electronic properties of hexagonal NbSe<sub>2</sub> and square BiSe layers that terminate the surface of the (BiSe)<sub>1+δ</sub>NbSe<sub>2</sub> misfit compound. We show that the band structure in the BiSe layers is strongly affected by the presence of the hexagonal NbSe<sub>2</sub> layers, leading to quasi-one-dimensional electronic features. The electronic structure of the NbSe<sub>2</sub> layers, on the other hand, is hardly influenced by the presence of the BiSe. Using density functional theory calculations of the unfolded band structures, we argue that the preferred modification of one type of band is mainly due to the atomic and orbital character of the states involved, opening a promising way to design electronic states that exploit the partially incommensurate character of the misfit compounds.

DOI: [10.1103/PhysRevMaterials.6.L092001](https://doi.org/10.1103/PhysRevMaterials.6.L092001)

A stack of two-dimensional (2D) materials bound by van der Waals forces is naively not expected to show strong interlayer interactions, aside from a possible charge transfer, especially when the two crystal lattices do not have the same unit cell or orientation [1]. However, precisely systems of this category have shown extremely rich physics caused by the formation of moiré lattices, band replicas, and flat bands [2–5], or even merely by the relative position of high-symmetry points that can strongly affect the stack's excitonic properties [6].

A similar situation could be expected in the so-called misfit compounds [7,8]. These are stacks of alternating 2D square and hexagonal lattices that result in a structure which is commensurate in one direction but incommensurate along the perpendicular direction in the plane of the 2D layers [see Fig. 1(a)]. The lack of commensurability prevents the formation of interlayer chemical bonds, but charge transfer between the layers can be substantial and can help stabilize the misfit compounds [9–11]. An electronic interlayer interaction beyond charge transfer has so far not been reported. However, it is well-known that the two layers are affected by each other's presence such that the lattice structure of each layer is modulated by the periodicity of the other layer [7,12], something that ought to be manifest also in the electronic

structure. One might ask whether misfit crystals can exhibit phenomena analogous to, e.g., twisted bilayer graphene. However, the misfit compounds are different from most of the artificial stacks of 2D materials studied so far [13–15] in the sense that the latter usually combine two hexagonal lattices, whereas a misfit structure consists of hexagonal and square lattices.

Here we study the (BiSe)<sub>1+δ</sub>NbSe<sub>2</sub> misfit compound. The structure shown in Fig. 1(a) is a stack of square BiSe layers and hexagonal NbSe<sub>2</sub> layers (slightly deformed such that there is commensurability in the *y* direction). Based on transport data, charge transfer is not expected to play a major role in this compound [9,16]. The material is superconducting with a *T<sub>c</sub>* around 2.4 K [17–19], and an argument has been made that the superconductivity does not have the 2D character of a NbSe<sub>2</sub> intercalation compound but is rather of a three-dimensional nature [17]. We characterize the samples using angle-resolved photoemission spectroscopy (ARPES) with a small light focus, giving us the possibility to individually probe the electronic structure of different surface terminations (by BiSe or NbSe<sub>2</sub> layers) and thereby to draw conclusions about the misfit structure's effect on the individual layers. The experimental findings suggest a hitherto unobserved interlayer interaction, leading to the emergence of one-dimensional (1D) features in the electronic structure. They are supported by density functional theory (DFT) calculations.

\*philip@phys.au.dk

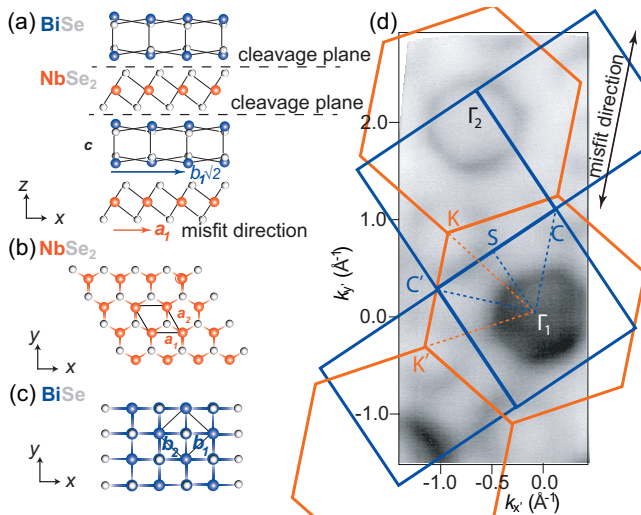


FIG. 1. (a) Side-view of the  $(\text{BiSe})_{1+\delta}\text{NbSe}_2$  misfit compound. Dashed lines indicate possible cleavage planes. The incommensurate direction is labeled misfit direction. (b), (c) Top view of the structure's  $\text{NbSe}_2$  and  $\text{BiSe}$  layers with the unit cells indicated. (d) Photoemission intensity at the Fermi energy (high intensity is dark) taken at 65 eV photon energy with the 2D Brillouin zones for square  $\text{BiSe}$  and hexagonal  $\text{NbSe}_2$  superimposed. The corners of the  $\text{BiSe}$  Brillouin zone are called C and C' to account for the broken symmetry.

$(\text{BiSe})_{1+\delta}\text{NbSe}_2$  misfit crystals with a superconducting  $T_c$  of 2.2 K were grown following the procedure given by Nagao *et al.* [18], using a nominal  $\delta = 0.4$ . Different choices of  $0.1 < \delta < 0.4$  gave the same  $T_c$  and the same peak positions from the misfit phase in x-ray diffraction. Conventional ARPES experiments were performed at the SGM-3 beamline of ASTRID2 [20] and small-spot (microARPES) measurements were carried out at the I05 beamline of Diamond Light Source (DLS). The light spot size was on the order of  $200/5 \mu\text{m}$  at ASTRID2/DLS and linear horizontal polarization was used. The sample temperature was 45/55 K; energy and angular resolution were 35/30 meV and  $0.2^\circ$ . The photon energy is given in the figures. Electronic structure calculations for individual  $\text{BiSe}$  and  $\text{NbSe}_2$  layers as well as for a commensurate approximation to the misfit structure were performed using the VIENNA AB INITIO SIMULATION PACKAGE (VASP) [21,22]. Unfolding calculations were performed using the new patch version of VASP (UnfoldingPatch4vasp) and B4VASP packages [23]. Details about structural relaxation and the band structure unfolding are given in the Supplemental Material (SM) [24], see also Refs. [25–32].

The misfit structure shown in Fig. 1(a) is preferentially cleaved between the 2D layers, resulting in a surface that is either terminated by  $\text{NbSe}_2$  or by  $\text{BiSe}$ , as shown Figs. 1(b) and 1(c). Due to the surface sensitivity of ARPES, the photoemission intensity is expected to be dominated by the topmost layer. However, when a sufficiently large surface area is probed, both terminations are expected to be present in equal amounts. Figure 1(d) shows the photoemission intensity at the Fermi level  $E_F$ , obtained using a large UV light spot ( $\approx 100 \times 190 \mu\text{m}^2$ ), presumably averaging over the two different surface terminations. The result strongly resembles

ARPES results from  $\text{NbSe}_2$  [33–38], with the characteristic hole pockets around the  $\Gamma$  and K points of the hexagonal Brillouin zone (BZ). Superficially, no distinct features obviously stemming from the  $\text{BiSe}$  layers are visible. While surprising, this is consistent with recent ARPES studies of similar misfit compounds that did not reveal *any* sign of the cubic layers' electronic structure [10,11]. However, upon closer inspection, we note that the hexagonal hole pocket around  $\Gamma_1$  appears filled and thereby distinctly different from the one in the neighboring BZ around  $\Gamma_2$  and from that expected for  $\text{NbSe}_2$  [33]. As we shall see below, this is in fact a contribution of the  $\text{BiSe}$  layers.

From the size of the  $\text{NbSe}_2$  Fermi contour, we can determine an additional band filling of  $0.26 \pm 0.01$  electrons per  $\text{NbSe}_2$  unit cell compared to the charge-neutral single-layer [24]. This is consistent with a charge transfer between the layers and with a relative shift of the bands in the calculated electronic structure of the misfit approximant; see SM [24]. Note, however, that without an independent measurement of the  $\text{BiSe}$  Fermi contour, it is not possible to disentangle a charge transfer between the layers from a possible overall doping of the sample, something that could arise from the formation of nonstoichiometric defects [39].

A more detailed insight into the termination-dependent electronic structure is gained by scanning a highly focused ( $\approx 5 \mu\text{m}$ ) UV beam across the surface, such that regions with a unique surface termination are resolved [see Figs. 2(a) and 2(b)]. When performing such a scan over an area of  $43 \times 40 \mu\text{m}^2$ , we find the electronic structure to be dominated by the two types of dispersion shown in Figs. 2(c) and 2(d), which we ascribe to the two surface terminations ( $\text{NbSe}_2$  and  $\text{BiSe}$ ). Assigning the type of termination is achieved by a comparison to DFT calculations for isolated single layers of  $\text{NbSe}_2$  and  $\text{BiSe}$  [Figs. 2(e) and 2(f), respectively] [24]. The electronic structure of the two layers is sufficiently different for this to be straightforward: For  $\text{NbSe}_2$ , the  $\Gamma$  point is encircled by a hole pocket as shown in Figs. 2(c) and 2(e) (marked by green arrows).  $\text{BiSe}$  also shows a hole pocket around  $\Gamma$  but with the simultaneous presence of an occupied electronlike band, as seen in Figs. 2(d) and 2(f) [the bands giving rise to the hole pocket are also marked in Fig. 2(f)]. Since ARPES does not exclusively probe the first layer and since the spatial resolution is limited, the electron band is also faintly visible for the  $\text{NbSe}_2$  termination, but it is much weaker. Figure 2(b) shows the photoemission intensity in a region of interest around this electron band, marked by a rectangle in Fig. 2(d), and high intensity therefore indicates the presence of the  $\text{BiSe}$  termination. The clear distinction between the two surface terminations is also supported by mapping their qualitatively different core level spectra, as discussed in the SM [24].

While a detailed inspection of the  $\text{NbSe}_2$ -terminated regions gives results that are very similar to bulk  $\text{NbSe}_2$  crystals or single layers, apart from the aforementioned strong doping effects [33–38] (see SM [24]), the results from the  $\text{BiSe}$ -terminated parts are more complex. The photoemission intensity at  $E_F$ , as well as along cuts throughout the 2D square BZ, is shown in Figs. 3(a) and 3(b), respectively. The characteristic features of the  $\text{NbSe}_2$  termination are still dominating. However, and in contrast to the results of Refs. [10,11], we also find photoemission features that do not originate from

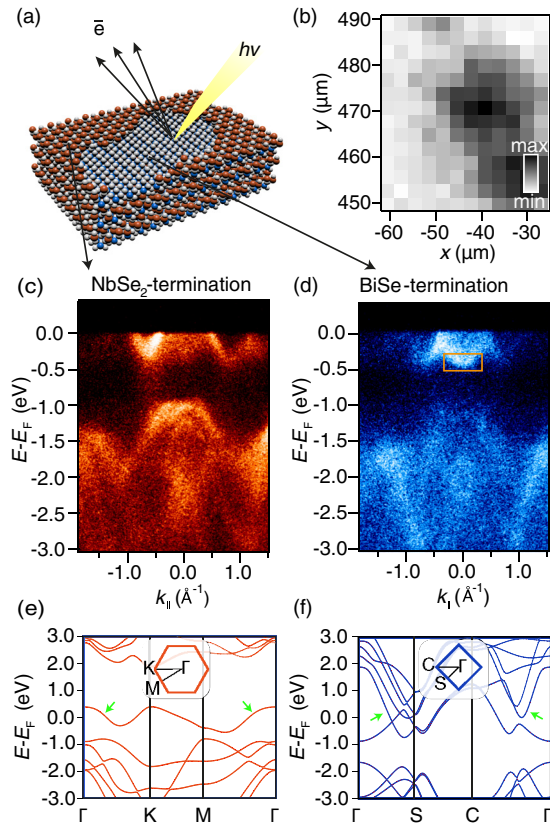


FIG. 2. (a) Sketch of the experimental geometry. A highly focused UV beam is scanned across the surface of the misfit compound, leading to photoemission from only one of the two possible terminations of the crystal. (b) Map of the  $(x, y)$ -dependent photoemission intensity integrated over the rectangular region of interest in panel (d). (c), (d) Distinctly different spectra collected at 133 eV photon energy from NbSe<sub>2</sub> and BiSe surface terminations. (e), (f) Calculated electronic structure for an isolated 2D layer of NbSe<sub>2</sub> and BiSe, respectively. The 2D BZs are shown as insets. The green arrows mark the bands leading to hole pockets around  $\Gamma$ .

the NbSe<sub>2</sub> layers, such as the aforementioned electron band around the  $\Gamma$  point. It has a similar dispersion as in the calculation of Fig. 2(f) but it is less occupied, also supporting a charge transfer from BiSe to NbSe<sub>2</sub>. Moreover, this dispersion is smeared out in all directions, explaining the filled character of the Fermi contour around  $\Gamma$ . Further out toward the BZ boundary, there is a downward dispersing band forming a holelike Fermi contour, also in good agreement with the calculation, see arrows in Fig. 2(f). Due to the simultaneously present photoemission intensity from the NbSe<sub>2</sub>, what are observed are actually two superimposed hole pockets, seen near the arrows in Fig. 3(b) and in more detail in the SM [24]. No replicas of the electron band can be found around higher reciprocal lattice vectors of the square BiSe lattice.

The most interesting features observed on the BiSe termination are 1D lines of strong photoemission intensity at  $E_F$  [marked by arrows in Fig. 3(a)]. Similar structures also appear at higher binding energies and we can exploit their 1D nature to identify the incommensurate (misfit) direction (see SM [24]). The 1D lines resemble those typically found for nearly 1D materials [40] and they do not appear in any of the

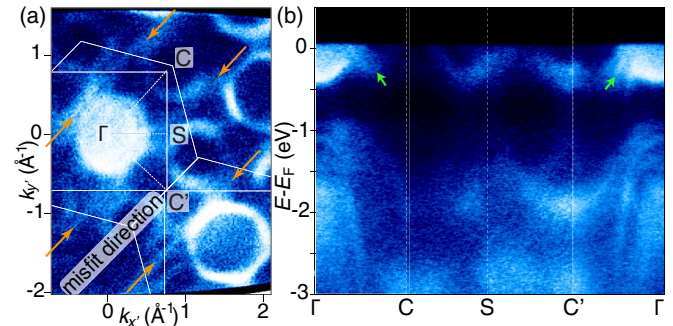


FIG. 3. (a) Photoemission intensity at the Fermi level recorded at 133 eV photon energy for the BiSe termination. The orange arrows mark one-dimensional lines of high photoemission intensity in the misfit direction. (b) Dispersion in the square Brillouin zone of BiSe. The green arrows mark the dispersion from two hole pockets, one from BiSe and one from NbSe<sub>2</sub>.

misfit structure's constituent layers on their own, so evidently they manifest a hitherto unseen interlayer interaction that goes beyond charge transfer.

A plausible explanation for these observations arises from the structural interaction between the 2D materials in the misfit compound, as well as from the orbital character of the bands near  $E_F$ . The interaction between the 2D sheets causes each to be distorted in a nonperiodic fashion. In a misfit crystal of composition MX TX<sub>2</sub>, the modulation-induced deformation is typically highest for the atoms at the interface, i.e., the entire MX layer and the X atoms from TX<sub>2</sub>, while the T atoms in the TX<sub>2</sub> layers are least affected [7,12,41,42]. This explains why the NbSe<sub>2</sub> Fermi contour, which is formed from Nb 3d orbitals, is hardly influenced by the formation of the misfit compound. Interestingly, even the deeper lying Se-derived bands around 1 eV below  $E_F$  are still very similar to those in single-layer NbSe<sub>2</sub> [36], suggesting that the entire NbSe<sub>2</sub> layer is little affected by the presence of the BiSe. The BiSe states near  $E_F$ , on the other hand, have Bi 6p character (see SM [24]) and are therefore susceptible to the changed electronic environment of the Bi atoms as well as to the loss of periodicity in the misfit direction. The resulting electronic structure of BiSe near  $E_F$  will thus no longer be periodic in the misfit direction. These considerations can explain the absence of a periodicity following the square BiSe reciprocal lattice and the emergence of a 1D electronic structure.

We support these arguments by DFT calculations. To understand the formation of the 1D structures at  $E_F$ , we start by inspecting the Fermi contours for freestanding layers of NbSe<sub>2</sub> and BiSe, with the lattice parameters constrained to the value found for the misfit approximant. The superposition of the two contours is shown in Fig. 4(a). It would represent the Fermi contour of the misfit compound in the absence of any interlayer interaction and charge transfer, with each Fermi contour repeated according to its reciprocal lattice. Clearly, this is not supported by the experiment. For a more appropriate description, and given the experimental evidence of a hardly affected NbSe<sub>2</sub> band structure, we start to approximate the misfit structure by a rigid NbSe<sub>2</sub> layer and ask how its periodic potential affects the electronic structure of the neighboring BiSe layers or the electronic structure of

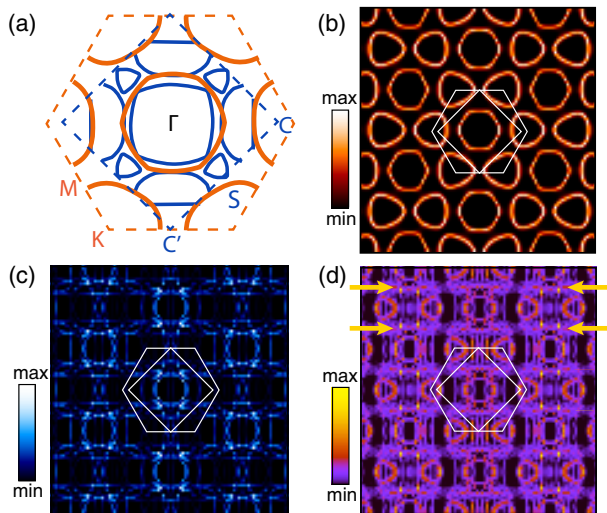


FIG. 4. (a) Calculated Fermi contour for freestanding NbSe<sub>2</sub> and BiSe layers, using the experimentally determined Fermi level. (b) Spectral function near  $E_F$  for NbSe<sub>2</sub> in the approximate unit cell of the misfit structure, unfolded onto the primitive NbSe<sub>2</sub> reciprocal lattice. (c), (d) Corresponding spectral functions unfolded on the primitive NbSe<sub>2</sub> lattice for freestanding BiSe and the complete misfit structure. The arrows mark the position of one-dimensional features in the electronic structure.

the combined misfit crystal. To this end, we calculate the electronic structure of a NbSe<sub>2</sub> and a BiSe layer, as well as a (BiSe)<sub>1.14</sub>NbSe<sub>2</sub> misfit approximant in a commensurate unit cell of 7 NbSe<sub>2</sub> and  $8/\sqrt{2}$  BiSe lattice vectors along the misfit direction. We then unfold the electronic structure calculated in this supercell onto the primitive unit cell of NbSe<sub>2</sub>—see SM [24].

The spectral functions near the Fermi energy resulting from the band unfolding (for a definition, see SM [24]) are given in Figs. 4(b)–4(d). For a large supercell just containing NbSe<sub>2</sub>, the unfolding on the primitive cell in Fig. 4(b) merely gives the expected Fermi contour of this layer. For a single layer of BiSe and for the misfit approximant, the result is more complex [see Figs. 4(c) and 4(d)], but in both cases, one can readily make out 1D features along the misfit direction, similar to those observed in the experiment. This is especially pronounced for the unfolded electronic bands of the misfit approximant (marked by arrows). The origin of the 1D structure is a complex interplay of lost translational symmetry and interlayer interaction. The original electronic structure elements responsible for the lines are the straight sides of the hexagonal hole pocket around  $\Gamma$  for NbSe<sub>2</sub>, as well as the almost straight lines of the electron (hole) pockets in BiSe. These two features interact strongly, i.e., they are not simply superimposed, as can be seen by comparing the unfolded band structure of the misfit approximant with those of the individual single layers, and as is also plausible considering their predominant orbital character (Bi  $p_z$  and Nb  $d_{z^2}$ ) [24].

The basic assumption of the calculations is a fairly rigid NbSe<sub>2</sub> template, imposing its structure onto the BiSe layer and thereby justifying the choice of projecting the bands onto the NbSe<sub>2</sub> lattice. This is based on structural arguments and on the finding from ARPES that the NbSe<sub>2</sub> band structure is almost unaffected by the presence of BiSe, apart from charge transfer. This view is not only supported by the formation of the 1D structures but also by the continuous presence of the NbSe<sub>2</sub> hole pockets around the K points in Fig. 4(d). These pockets are placed in an area where there are few BiSe states available for hybridization and they are thus unaffected by the misfit structure, merely shrinking a little due to the charge transfer. Note that the full effect of the incommensurate structure can, of course, not be captured in a periodic calculation with a large but commensurate unit cell, nor can additional factors that could lead to 1D behavior, such as a longer-range modulation in the BiSe layer observed by electron microscopy [19]. Another candidate for creating a 1D confinement are Bi antiphase domain boundaries, also observed in the BiSe layer [43], but this type of defect does not appear to be common when following the synthesis method of Ref. [19], which is similar to the one also used here [18].

The misfit-induced transition from a 2D electronic structure to a 1D situation in the BiSe layers could have several interesting consequences. By definition, it effectively localizes the electrons in the incommensurate direction, preventing metallic transport through the BiSe layer in that direction. This is consistent with earlier findings in transport experiments, where an electron localization due to the incommensurate potential has been invoked to explain the fact that only the TS<sub>2</sub> layers contribute to the electric conductivity of some rare earth-based misfit compounds [44–46]. The creation of the 1D Fermi contour could further give rise to the rich physics expected in such situations, potentially giving rise to Peierls distortions, spin-charge separation, or the formation of Luttinger liquid states.

In summary, we have shown that the incommensurate interlayer interaction in the (BiSe)<sub>1+ $\delta$</sub> NbSe<sub>2</sub> misfit compound leads to a dimensionality reduction of the electronic structure in the square BiSe lattice, from a 2D to a 1D metallic state. This can explain earlier transport experiments in this class of materials that have found conductivity to be located exclusively in the transition metal dichalcogenide layer. It opens the possibility to realize 1D physics in this class of naturally occurring stacks of layered materials, exploiting the design freedom where doping, charge transfer, and the mechanical properties of the constituent layers can be widely tuned.

This work was supported by VILLUM FONDEN via the Centre of Excellence for Dirac Materials (Grant No. 11744) and the Independent Research Fund Denmark (Grant No. 1026-00089B). We acknowledge Diamond Light Source for time on Beamline I05 under Proposal No. SI25201-2. We thank Richard Balog, Kimberly Hsieh, and Jeppe Vang Lauritzen for discussions and technical support.

[1] A. K. Geim and I. V. Grigorieva, *Nature (London)* **499**, 419 (2013).

[2] R. Bistritzer and A. H. MacDonald, *Proc. Natl. Acad. Sci.* **108**, 12233 (2011).

- [3] Y. Cao, V. Fatemi, A. Demir, S. Fang, S. L. Tomarken, J. Y. Luo, J. D. Sanchez-Yamagishi, K. Watanabe, T. Taniguchi, E. Kaxiras *et al.*, *Nature (London)* **556**, 80 (2018).
- [4] E. Y. Andrei and A. H. MacDonald, *Nat. Mater.* **19**, 1265 (2020).
- [5] A. J. H. Jones, R. Muzzio, S. Pakdel, D. Biswas, D. Curcio, N. Lanatà, P. Hofmann, K. M. McCreary, B. T. Jonker, K. Watanabe *et al.*, *2D Mater.* **9**, 015032 (2022).
- [6] J. Choi, M. Florian, A. Steinhoff, D. Erben, K. Tran, D. S. Kim, L. Sun, J. Quan, R. Claassen, S. Majumder *et al.*, *Phys. Rev. Lett.* **126**, 047401 (2021).
- [7] G. Wieggers, *Prog. Solid State Chem.* **24**, 1 (1996).
- [8] D. Merrill, D. Moore, S. Bauers, M. Falmbigl, and D. Johnson, *Materials* **8**, 2000 (2015).
- [9] G. Wieggers, *J. Alloys Compd.* **219**, 152 (1995).
- [10] Q. Yao, D. W. Shen, C. H. P. Wen, C. Q. Hua, L. Q. Zhang, N. Z. Wang, X. H. Niu, Q. Y. Chen, P. Dudin, Y. H. Lu *et al.*, *Phys. Rev. Lett.* **120**, 106401 (2018).
- [11] R. T. Leriche, A. Palacio-Morales, M. Campetella, C. Tresca, S. Sasaki, C. Brun, F. Debontridder, P. David, I. Arfaoui, O. Šofranko *et al.*, *Adv. Funct. Mater.* **31**, 2007706 (2021).
- [12] S. van Smaalen, *Phys. Rev. B* **43**, 11330 (1991).
- [13] F. Arnold, R.-M. Stan, S. K. Mahatha, H. E. Lund, D. Curcio, M. Dendzik, H. Bana, E. Travaglia, L. Bignardi, P. Lacovig *et al.*, *2D Mater.* **5**, 045009 (2018).
- [14] L. Bignardi, S. K. Mahatha, D. Lizzit, H. Bana, E. Travaglia, P. Lacovig, C. Sanders, A. Baraldi, P. Hofmann, and S. Lizzit, *Nanoscale* **13**, 18789 (2021).
- [15] S. Kraus, F. Huttmann, J. Fischer, T. Knispel, K. Bischof, A. Herman, M. Bianchi, R.-M. Stan, A. J. Holt, V. Caciuc *et al.*, *Phys. Rev. B* **105**, 165405 (2022).
- [16] W. Zhou, A. Meetsma, J. de Boer, and G. Wieggers, *Mater. Res. Bull.* **27**, 563 (1992).
- [17] A. Nader, A. Briggs, and Y. Gotoh, *Solid State Commun.* **101**, 149 (1997).
- [18] M. Nagao, A. Miura, Y. Horibe, Y. Maruyama, S. Watauchi, Y. Takano, and I. Tanaka, *Solid State Commun.* **321**, 114051 (2020).
- [19] M. E. Kamminga, M. Batuk, J. Hadermann, and S. J. Clarke, *Commun. Mater.* **1**, 82 (2020).
- [20] S. V. Hoffmann, C. Søndergaard, C. Schultz, Z. Li, and P. Hofmann, *Nucl. Instrum. Meth. Phys. Res. Sect. A* **523**, 441 (2004).
- [21] G. Kresse and J. Furthmüller, *Comput. Mater. Sci.* **6**, 15 (1996).
- [22] G. Kresse and D. Joubert, *Phys. Rev. B* **59**, 1758 (1999).
- [23] D. Dirnberger, G. Kresse, C. Franchini, and M. Reticcioli, *J. Phys. Chem. C* **125**, 12921 (2021).
- [24] See Supplemental Material at <http://link.aps.org/supplemental/10.1103/PhysRevMaterials.6.L092001> for details on termination-dependent ARPES results, calculational details, the orbital character of the bands in the single layers, unfolded band structures, and the charge transfer within the misfit compound.
- [25] J. P. Perdew, K. Burke, and M. Ernzerhof, *Phys. Rev. Lett.* **77**, 3865 (1996).
- [26] J. P. Perdew, J. A. Chevary, S. H. Vosko, K. A. Jackson, M. R. Pederson, D. J. Singh, and C. Fiolhais, *Phys. Rev. B* **46**, 6671 (1992).
- [27] M. Calandra, I. I. Mazin, and F. Mauri, *Phys. Rev. B* **80**, 241108(R) (2009).
- [28] P. Hofmann, I. Y. Sklyadneva, E. D. L. Rienks, and E. V. Chulkov, *New J. Phys.* **11**, 125005 (2009).
- [29] K. Momma and F. Izumi, *J. Appl. Crystallogr.* **44**, 1272 (2011).
- [30] A. S. Ngankeu, S. K. Mahatha, K. Guilloy, M. Bianchi, C. E. Sanders, K. Hanff, K. Rossnagel, J. A. Miwa, C. Breth Nielsen, M. Bremholm *et al.*, *Phys. Rev. B* **96**, 195147 (2017).
- [31] B. Shao, A. Eich, C. Sanders, A. S. Ngankeu, M. Bianchi, P. Hofmann, A. A. Khajetoorians, and T. O. Wehling, *Nat. Commun.* **10**, 180 (2019).
- [32] S. Grimme, J. Antony, S. Ehrlich, and H. Krieg, *J. Chem. Phys.* **132**, 154104 (2010).
- [33] S. V. Borisenko, A. A. Kordyuk, V. B. Zabolotnyy, D. S. Inosov, D. Evtushinsky, B. Büchner, A. N. Yaresko, A. Varykhalov, R. Follath, W. Eberhardt *et al.*, *Phys. Rev. Lett.* **102**, 166402 (2009).
- [34] D. J. Rahn, S. Hellmann, M. Kalläne, C. Sohr, T. K. Kim, L. Kipp, and K. Rossnagel, *Phys. Rev. B* **85**, 224532 (2012).
- [35] F. Weber, R. Hott, R. Heid, L. L. Lev, M. Caputo, T. Schmitt, and V. N. Strocov, *Phys. Rev. B* **97**, 235122 (2018).
- [36] Y. Nakata, K. Sugawara, S. Ichinokura, Y. Okada, T. Hitosugi, T. Koretsune, K. Ueno, S. Hasegawa, T. Takahashi, and T. Sato, *npj 2D Mater. Appl.* **2**, 12 (2018).
- [37] C.-Z. Xu, X. Wang, P. Chen, D. Flötotto, J. A. Hlevyack, M.-K. Lin, G. Bian, S.-K. Mo, and T.-C. Chiang, *Phys. Rev. Mater.* **2**, 064002 (2018).
- [38] P. Dreher, W. Wan, A. Chikina, M. Bianchi, H. Guo, R. Harsh, S. Mañas-Valero, E. Coronado, A. J. Martínez-Galera, P. Hofmann *et al.*, *ACS Nano* **15**, 19430 (2021).
- [39] E. Kabliman, P. Blaha, and K. Schwarz, *Phys. Rev. B* **82**, 125308 (2010).
- [40] M. Grioni, S. Pons, and E. Frantzeskakis, *J. Phys.: Condens. Matter* **21**, 023201 (2009).
- [41] S. van Smaalen, *J. Phys.: Condens. Matter* **3**, 1247 (1991).
- [42] V. Petříček, I. Cisarova, J. L. de Boer, W. Zhou, A. Meetsma, G. A. Wieggers, and S. van Smaalen, *Acta Crystallogr.* **B49**, 258 (1993).
- [43] G. Mitchson, M. Falmbigl, J. Ditto, and D. C. Johnson, *Inorg. Chem.* **54**, 10309 (2015).
- [44] K. Suzuki, T. Kondo, T. Enoki, and S. Bandow, *Synth. Met.* **56**, 1741 (1993).
- [45] S. Aubry and G. André, *Ann. Israel Phys. Soc* **3**, 133 (1980).
- [46] M. Kohmoto, *Phys. Rev. Lett.* **51**, 1198 (1983).